ATP binding and hydrolysis disrupt the high-affinity interaction between the heme ABC transporter HmuUV and its cognate substrate-binding protein

Received for publication, February 8, 2017, and in revised form, July 10, 2017 Published, Papers in Press, July 14, 2017, DOI 10.1074/jbc.M117.779975

Hiba Qasem-Abdullah, Michal Perach, Nurit Livnat-Levanon, and Oded Lewinson[1]

From the Department of Biochemistry, The Bruce and Ruth Rappaport Faculty of Medicine, The Technion-Israel Institute of Technology, Haifa 31096, Israel

Edited by Thomas Söllner

Using the energy of ATP hydrolysis, ABC transporters catalyze the trans-membrane transport of molecules. In bacteria, these transporters partner with a high-affinity substrate-binding protein (SBP) to import essential micronutrients. ATP binding by Type I ABC transporters (importers of amino acids, sugars, peptides, and small ions) stabilizes the interaction between the transporter and the SBP, thus allowing transfer of the substrate from the latter to the former. In Type II ABC transporters (importers of trace elements, *e.g.* vitamin B_{12}, heme, and iron-siderophores) the role of ATP remains debatable. Here we studied the interaction between the *Yersinia pestis* ABC heme importer (HmuUV) and its partner substrate-binding protein (HmuT). Using real-time surface plasmon resonance experiments and interaction studies in membrane vesicles, we find that in the absence of ATP the transporter and the SBP tightly bind. Substrate in excess inhibits this interaction, and ATP binding by the transporter completely abolishes it. To release the stable docked SBP from the transporter hydrolysis of ATP is required. Based on these results we propose a mechanism for heme acquisition by HmuUV-T where the substrate-loaded SBP docks to the nucleotide-free outward-facing conformation of the transporter. ATP binding leads to formation of an occluded state with the substrate trapped in the trans-membrane translocation cavity. Subsequent ATP hydrolysis leads to substrate delivery to the cytoplasm, release of the SBP, and resetting of the system. We propose that other Type II ABC transporters likely share the fundamentals of this mechanism.

ATP -binding cassette (ABC)[2] transporters comprise a large superfamily of membrane proteins. From bacteria to man, they transport molecules through the permeability barriers of cell membranes (1–4). Cargo molecules are extremely diverse, ranging from ions, small to medium molecules (sugars, amino acids, lipids, and ionic metals) to large and bulky compounds (peptides, proteins, organo-metal complexes, and antibiotics). They are involved in many important physiological processes such as nutrient import, cellular detoxification, lipid homeostasis, signal transduction, antiviral defense, and antigen presentation (5–11). From a clinical perspective, ABC transporters are of great interest as they are directly involved in tumor resistance to multiple chemotherapeutics, bacterial multidrug resistance, and bacterial virulence and pathogenesis (12–19). All ABC transporters share a basic architecture, minimally composed of two intracellular nucleotide-binding domains (NBDs), and two trans-membrane domains (TMDs). The NBDs supply the energy via ATP binding and hydrolysis, and the TMDs form the trans-membrane permeation pathway. ABC transporters that function as importers additionally require a substrate-binding protein (SBP) that binds the substrate outside the cytoplasm and delivers it to the TMDs (20–24). In recent years it has become apparent that despite the common basic architecture there is a considerable degree of structural and mechanistic diversity within the large family of ABC transporters (25–29). One mechanistic aspect of the transport cycle concerns the role of ATP binding and hydrolysis. In Type I transporters (importers of common metabolites, *e.g.* sugars and amino acids (30–32)), and in exporters, ATP binding induces conversion to an outward-facing conformation of the transporter, and promotes a stable interaction with the cognate SBP (33, 34). In Type II transporters (importers of trace organo-metal complexes, *e.g.* iron-siderophores, vitamin B_{12}, and heme) the role of ATP is not as clear, as different experimental setups lead to different conclusions (34–38).

Here, we studied the role of ATP binding and hydrolysis in the Type II heme transporter HmuUV-T of *Yersinia pestis* (39–41). Using surface plasmon resonance and interaction experiments performed in membrane vesicles, we observe that in HmuUV-T, ATP has a role that is very different from that described in Type I systems.

Results

Specificity of the HmuUV-HmuT interaction

Structural studies of the Type II ABC transporters BtuCD, MolBC, BhuUV, and HmuUV show that their structures are very similar (38, 41–43). Superimposition of the nucleotide-free, outward-facing structures of BtuCD and HmuUV lends the impression of different conformations of a single protein

This work was supported in part by grants from the Rappaport Family Institute for biomedical research (to O. L.), the Merieux research foundation (to O. L.), and NATO Science for Peace Grant SPS-984622 (to O. L.). The authors declare that they have no conflicts of interest with the contents of this article.

This article contains supplemental Figs. S1–S3.

[1] To whom correspondence should be addressed. Tel.: 972-4-8295428; Fax: 972-4-8295205; E-mail: lewinson@tx.technion.ac.il.

[2] The abbreviations used are: ABC, ATP-binding cassette; NBD, nucleotide-binding domain; TMD, trans-membrane domain; SBP, substrate-binding protein; SPR, surface plasmon resonance; AMP-PNP, 5′-adenylyl-β,γ-imidodiphosphate.

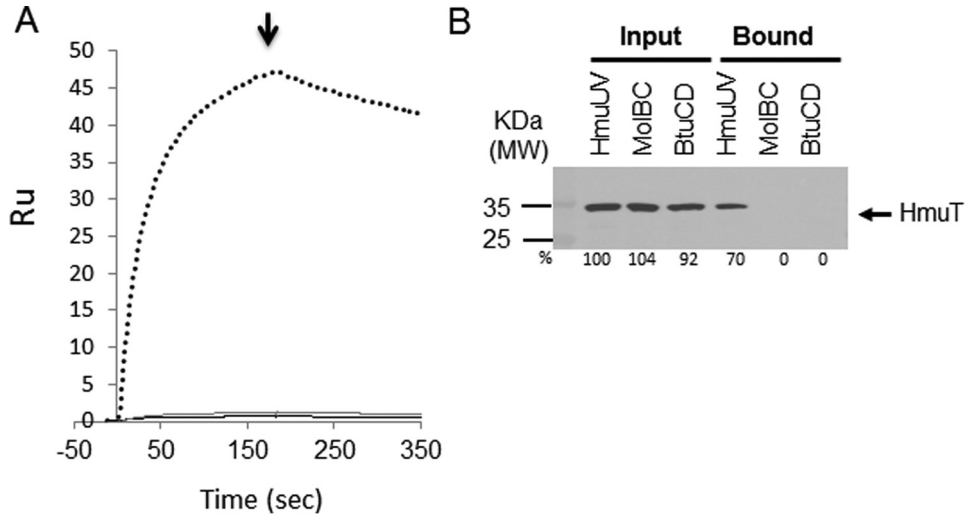

Figure 1. HmuT binds specifically to HmuUV. *A*, SPR sensograms showing the injection of 100 nM FLAG-HmuT over HmuUV (*dotted black curve*), BtuCD (*solid gray curve*), and MolBC (*solid black curve*) immobilized on adjacent flow cells. The *arrow* marks the end of the FLAG-HmuT injection and the onset of washing the biosensor chip with buffer. Shown are representative results of experiments conducted three times in duplicates (technical repeats). *B*, complex formation in the membrane environment: membranes were prepared from *E. coli* cells overexpressing HmuUV, MolBC, or BtuCD, as indicated. Following incubation with 50 nM FLAG-HmuT and subsequent washing, membrane-bound FLAG-HmuT was visualized by SDS-PAGE and Western blotting using an α-FLAG antibody. The *numbers below each lane* are the quantification with Total lab software, given as percent. Shown are representative results of three biological repeats.

rather than two different proteins (supplemental Fig. S1*A*). Similarly, the structures of the cognate SBPs (BtuF, HmuT, and MolA) also superimpose extremely well (supplemental Fig. S1*B*). In addition, in all three systems the glutamate-arginine pairs (responsible for the SBP-transporter interactions) are identically located (41, 44). We therefore began by examining the specificity of the transporter-SBP interaction. For this we used surface plasmon resonance experiments (SPR), as we have done in the past with several other ABC import systems (34, 35). In these experiments the His-tagged transporter is immobilized onto a nickel-nitrilotriacetic acid biosensor chip and the SBP is injected into the overflowing buffer. The interaction is recorded in real time and with high sensitivity. We immobilized equal amounts (by mass) of HmuUV, BtuCD, and MolBC onto adjacent flow cells of a biosensor chip and then injected HmuT over the transporters. As shown in Fig. 1*A*, HmuT robustly associated only with HmuUV and not with either BtuCD or MolBC. The SPR experiments are conducted in a detergent solution environment that is different from the native membrane. We and others have observed in the past that the detergent environment is a reasonable membrane mimic, yet some mechanistic features are only maintained in the native environment (34, 35, 45–47). We therefore tested whether the high specificity of the HmuUV-T interaction is also manifested in the membrane environment. For this we overexpressed HmuUV, MolBC, and BtuCD in *Escherichia coli* cells and prepared membrane fractions. We then incubated the membranes with HmuT, pelleted them, washed them with buffer, and analyzed the association of HmuT with the membranes using SDS-PAGE and Western blotting. We found that HmuT stably associated to membranes prepared from HmuUV expressing cells, and no such association was observed with membranes prepared from cells expressing either BtuCD or MolBC (Fig. 1*B*). Taken together, these results show that the HmuUV-HmuT interaction is specific, and that despite the high structural similarity there is no cross-reactivity between the transporters and non-cognate SBPs.

Affinity and pre-equilibrium kinetics of the HmuUV-HmuT interaction

The HmuUV-T association experiments shown in Fig. 1 were performed in the absence of nucleotides. The slow dissociation rate of the complex (Fig. 1, 175–350 s) and the resilience of the complex to the wash step of the membrane association experiments suggest that nucleotide-free HmuUV forms a stable complex with apo HmuT. To determine the affinity and pre-equilibrium dynamics of HmuUV-T interaction we conducted SPR experiments where a series of apo HmuT concentrations were injected over a constant amount of HmuUV. From these experiments, we can derive the kinetic rate constants of the interaction, assuming a simple 1:1 interaction model that includes no other assumptions (see "Experimental procedures"). As shown in Fig. 2*A*, the interaction is of high affinity, with $K_D = 2.25 \times 10^{-9}$ M. The interaction has a relatively fast k_{on} for a protein-protein interaction of 6.18×10^5 M^{-1} s^{-1}, and a slow k_{off} of 1.56×10^{-3} s^{-1}. The nanomolar range affinity measured here for the HmuUV-T interaction is very similar to the affinity between the Type II ABC importer MolBC and its SBP ($K_D = 3 \times 10^{-9}$ M (34)), but is of significantly lower affinity than the ultra-stable picomolar affinity BtuCD-BtuF interaction (35). To determine whether the nanomolar range interaction affinity between HmuUV and HmuT also occurs in a membrane environment, we incubated HmuUV containing membranes with increasing concentrations of HmuT, pelleted the membranes, and estimated how much HmuT remained bound to the membrane fraction following a wash step. Fig. 2, *B* and *C*, shows such as experiment and demonstrates that half-maximal binding occurs at ~10 nM HmuT. Because of the detection range of the Western blot we were obliged to use a HmuUV concentration of ~25 nM.

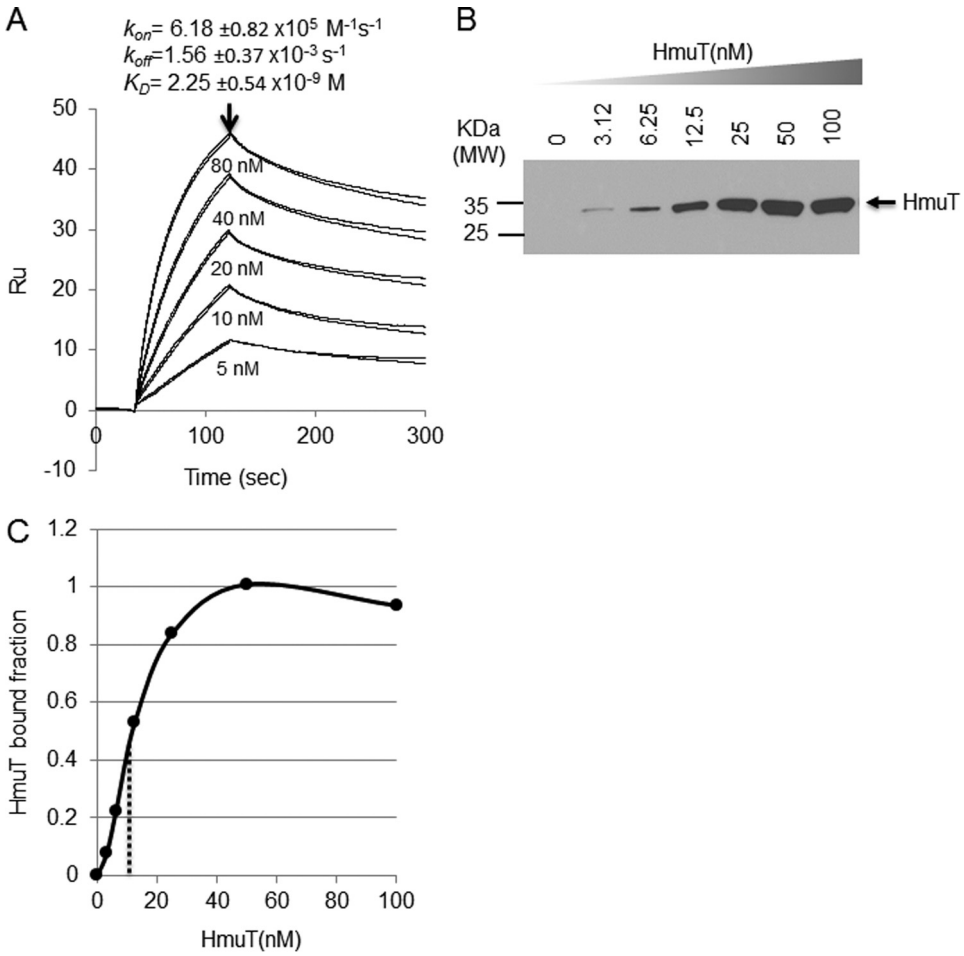

Figure 2. Dynamics of HmuUV-T complex formation. *A,* shown are duplicates of injections of the indicated concentrations of FLAG-HmuT over His-HmuUV immobilized onto a biosensor SPR chip. The *arrow* marks the end of the FLAG-HmuT injection and the onset of washing the biosensor chip with buffer. Also shown are the rate constants and their standard errors ($n = 3$) that were determined using a simple 1:1 interaction model. Shown are the representative results of experiments conducted three times in duplicates (technical repeats). *B,* complex formation in a native environment. Membranes were prepared from *E. coli* cells overexpressing HmuUV and incubated with the indicated concentrations of FLAG-HmuT. Following a wash step, the amount of membrane-associated HmuT was visualized by SDS-PAGE and Western blotting using an α-FLAG antibody. Shown are representative results of three biological repeats. *C,* the Western blot shown in *B* was quantified by Total lab software, and plotted as a function of HmuT concentrations. The *dashed line* indicates the concentration of HmuT at which half-maximal binding was measured.

Because the concentration of HmuUV used in these experiments is greater than the estimated K_D of 10 nM, this means that the affinity is at least in the range of 10 nM, but might actually be higher. Collectively, the SPR and membrane association experiments show that unlike the Type I transporters MalFGK-E, ModBC-A, and MetIN-Q, but similar to the Type II transporters BtuCD-F, BhuUV-T, and MolBC-A (33–35, 38, 48, 49), nucleotide-free HmuUV forms a stable complex with apo HmuT.

Effects of the substrate, heme, on the interaction between HmuUV and HmuT

We and others (33–35, 50) have observed in the past that the substrates of ABC import systems greatly influence the interaction between the transporters and the SBPs, dramatically affecting both the equilibrium and pre-equilibrium rate constants. For example, in the Type I molybdate/tungstate import system ModBC-A the interaction was completely substrate dependent: no interaction occurs unless the SBP is substrate-bound (34). Similarly, to form a stable complex with the maltose transporter, the maltose-binding protein must be substrate-loaded (33, 50). In contrast, in Type II ABC importers, the highest affinity is observed in the absence of substrate, and high substrate concentrations can dramatically change the association/dissociation kinetics (BtuCD), or completely block the interaction (MolBC) (34, 35). To test the effect of heme on the HmuUV-T interaction we first verified that our HmuT is substrate-free (supplemental Fig. S2). We then injected a constant concentration of HmuT over immobilized HmuUV, in the presence of increasing concentrations of heme. At a 1:1 heme: HmuT molar ratio (100 nM), complex formation was inhibited by ~12%. This inhibition increased to ~75% at a 10:1 heme: HmuT molar ratio and an almost complete inhibition of complex formation was observed at a 100:1 ratio (Fig. 3*A*). Visual inspection of the dissociation phase observed in the presence of 1 μM heme suggests a faster k_{off} in the presence of high substrate concentrations, as has been demonstrated for the vitamin B_{12} ABC transporter BtuCD-F. However, the effects of high heme concentrations were not exhaustively studied due to technical limitations.

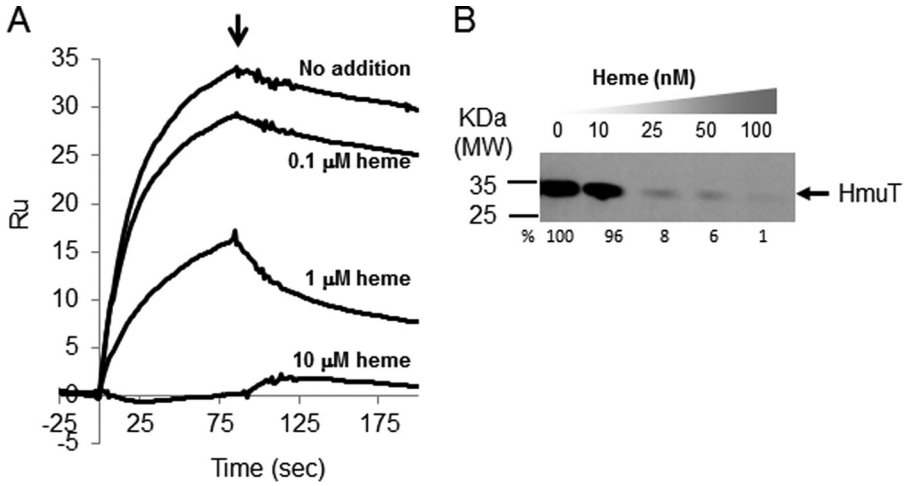

Figure 3. Effect of substrate on the interaction between HmuT and HmuUV. *A,* 100 nM FLAG-HmuT were injected over immobilized HmuUV in the absence or presence of the indicated concentrations of heme. The *arrow* marks the end of the FLAG-HmuT injection and the onset of washing the biosensor chip with buffer. Shown are the representative results of five technical repeats. *B,* 10 nM FLAG-HmuT was added to membranes prepared from *E. coli* cells overexpressing HmuUV in the absence or presence of the indicated heme concentrations. Bound FLAG-HmuT was visualized as shown in Figs. 1*B* and 2*B*. The *numbers below each lane* are the quantification with Total lab software, given as percent. Shown are representative results of four biological repeats.

The effect of heme on the formation the HmuUV-T complex was also studied in the membrane environment. Here also, addition of substrate at 1:1 heme:HmuT molar ratio did not greatly affect the interaction. As observed in the SPR experiments, higher substrate:SBP ratios completely disrupted the stable association between the transporter and the SBP.

Of note, substrate-induced inhibition of the HmuV-T interaction was only observed at heme:HmuT molar ratios greater than one. We therefore tentatively suggest that the second heme-binding event (which is of low affinity) serves as a negative feedback on transport.

The effects of the nucleotide state of HmuUV on its interaction with HmuT

In the Type I ABC transporters MalFGK and ModBC, ATP binding stabilizes the interaction with the SBP (34, 51). The opposite was shown for the Type II ABC transporters BtuCD (35), MolBC (34), and BhuUV (38). Conversely, Korkhov *et al.* (46) concluded that ATP binding to BtuCD stabilizes its interaction with BtuF.

We investigated the effect of ATP binding and hydrolysis on formation of the HmuUV-HmuT complex by conducting SPR experiments where HmuUV was trapped at its different nucleotide states (apo, ATP-bound, transition state, or ADP-bound). To ensure complete trapping of HmuUV in the different intermediate states, nucleotides were added at saturating concentrations (supplemental Fig. S3). To mimic the ATP-bound pre-hydrolysis state we added either ATP in the presence of low concentrations of EDTA, or AMP-PNP in the presence of magnesium. Under both conditions, we observed complete inhibition of the interaction between the transporter and the SBP (Fig. 4*A*).

Following binding of ATP, the bond in its γ-phosphate is cleaved by the NBDs, and a high energy catalytic intermediate is formed where the bond to the γ-phosphate is broken, yet the γ-phosphate has not yet been released from the ATP-binding site. To mimic this state, we incubated HmuUV in the presence of magnesium, ATP, and vanadate. Similar to what was observed in the ATP-bound state, the high-energy catalytic intermediate also showed no interaction with the SBP (Fig. 4*A*). Once the γ-phosphate was released from the ATP-binding site the transporter proceeds to its ADP-bound state, and to mimic this state we incubated HmuUV in the presence of magnesium and ADP. As shown in Fig. 4*A*, nearly complete restoration of the

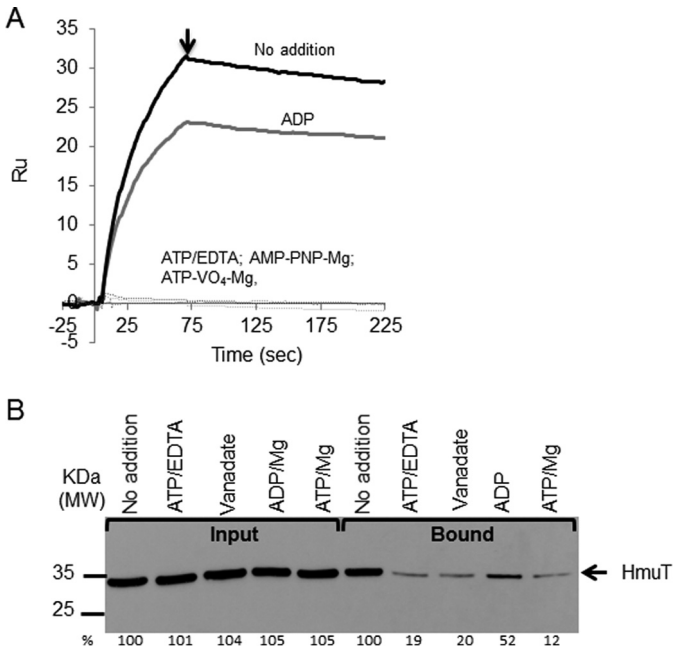

Figure 4. Effects of the nucleotide state of HmuUV on its interaction with HmuT. *A,* 100 nM HmuT was injected in the absence of nucleotides (*solid black curve*), or in the presence of ADP/Mg (*solid gray curve*), ATP-EDTA, AMP-PNP/Mg, or ATP-vanadate/Mg (indistinguishable *dotted curves*, as indicated). All nucleotides, vanadate, and magnesium were added at 1 mM, EDTA was added at 50 μM. The *arrow* marks the end of FLAG-HmuT injection and the onset of washing the biosensor chip with buffer. Shown are representative results of three technical repeats conducted in duplicates. *B*, effects of nucleotides in the membrane environment. The indicated nucleotides were incorporated to the lumen of the membrane vesicles, and then incubated with 250 nM FLAG-HmuT. Bound FLAG-HmuT was visualized as described in the legend to Figs. 1*B* and 2*B*. The *numbers below each lane* are the quantification with Total lab software, given as percent. Shown are representative results of three biological repeats.

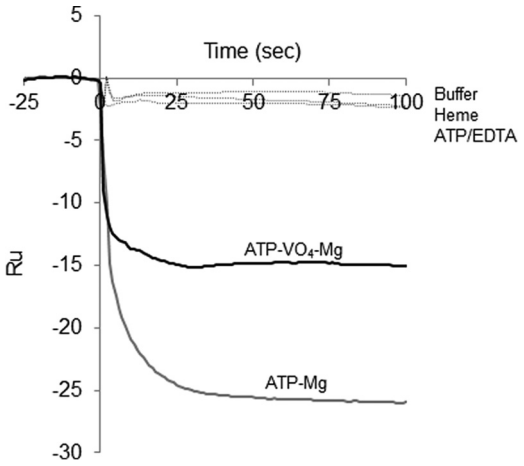

Figure 5. ATP hydrolysis triggers HmuUV-T dissociation. The pre-formed HmuUV-T complex was immobilized onto a biosensor chip and the indicated ligand was injected for 100 s in an attempt to dissociate the complex. Shown are the injections of 1 mM ATP, 1 mM $MgCl_2$ (*solid gray*); 1 mM ATP, 1 mM VO_4, 1 mM $MgCl_2$ (*solid black*); and in *dotted black* are the indistinguishable injections of 1 mM ATP, 50 μM EDTA, or 10 μM heme, or wash buffer. Shown are representative results of three technical repeats.

association with the SBP was observed when HmuUV was at the ADP-bound state. A similarly modest ADP-induced inhibition of complex formation was also observed in the homologous Type II ABC transporters BtuCD-F and MolBC-A (34, 35).

We next tested whether a similar pattern of nucleotide state-dependent interactions occurs in the membrane environment. For these experiments, we trapped the desired nucleotides in the lumen of the vesicles during their preparation (see "Experimental procedures") and then added HmuT externally. As shown in Fig. 4*B*, the results we obtained in the membrane vesicles were in excellent agreement with those obtained in the SPR experiments. The strongest and most stable association between HmuUV and HmuT was observed when HmuUV was nucleotide free, no association was observed in either the ATP-bound pre-hydrolysis or the vanadate-trapped high-energy states, and an intermediate level of binding was observed in the ADP-bound state.

Hydrolysis of ATP releases stably docked HmuT from HmuUV

As shown above, holo-HmuT stably docks to HmuUV, as long as there is no large excess of heme. The complex that is formed is of high affinity ($K_D = 2.25 \times 10^{-9}$ M), and has a very slow k_{off} of 1.56×10^{-3} s^{-1}. Such a slow k_{off} is incompatible with any reasonable prediction of the duration of the transport cycle. We therefore tested which conditions promote the dissociation of HmuT from HmuUV. For this, we first generated a stable HmuUV-T complex on an SPR chip and attempted to dissociate the complex using different ligands. The decrease in mass that accompanies dissociation of HmuT from HmuUV can be monitored in real time. Injection of a high concentration (10 μM) of heme had the same effect as the injection of buffer, and was completely unable to strip away any bound HmuT (Fig. 5). Interestingly, this (and even lower) concentration of heme dramatically inhibited complex formation when added simultaneously with HmuT, *i.e.* before allowing the complex to form (Fig. 3*A*). This observation is compatible with the notion that the substrate-binding pocket of the SBP is inaccessible when the latter is docked to the transporter. When added in concert with the SBP, ATP-EDTA (or AMP-PNP/Mg) completely inhibited the interaction of HmuT with HmuUV (Fig. 4, *A* and *B*). In contrast, when added post-complex, formation binding of ATP could not release the stably docked SBP. These observations suggest that if ATP binds to HmuUV before, or at the same time as HmuT, it prevents its docking to HmuUV. However, once the complex is formed binding of ATP is insufficient to dissociate the complex. Another possibility is that once the transporter-SBP complex has formed it has extremely low affinity to ATP. However, this is clearly not the case because when ATP is added to the preformed complex under hydrolyzing conditions (ATP-Mg), complex dissociation readily occurs (Fig. 5). Somewhat different observations were recently reported for the homologous heme ABC transporter BhuUV from *Burkholderia cenocepacia.* Here, binding of ATP was sufficient to trigger the release of the SBP (38). Interestingly, when ATP-Mg is added in the presence of vanadate, the amount of dissociated HmuT is (very reproducibly) half of that displaced in the fully hydrolyzing conditions (Fig. 5). The interpretation of this observation is discussed in the next section.

Discussion

Based on the results reported herein, and on the crystal structures of HmuUV and BtuCD, we propose a mechanistic model that may serve as a framework for future research (Fig. 6).

The X-ray structures of HmuUV and BtuCD suggest that they adopt an outward-facing conformation when they are nucleotide-free (41, 42). We demonstrate here that this nucleotide-free outward-facing conformation of HmuUV has the highest affinity to HmuT. When HmuUV is ATP-bound, or trapped in the transition state of ATP hydrolysis, we cannot detect any interaction with HmuT. Post-hydrolysis, after release of the inorganic phosphate (ADP-bound state), the HmuUV-T interaction affinity was almost completely restored. Notably, similar observations were made with three other Type II transporters (34, 35, 52). Based on these observations, we propose that the structure of the outward-facing nucleotide-free HmuUV (41) likely represents a transient physiological state of the transporter, to which HmuT preferentially binds (Fig. 6, *state I*). In the presence of stoichiometric substrate concentrations HmuT docks to HmuUV with very high (nM) affinity, and a stable complex is formed (Fig. 6, *state II*). When substrate is present at higher concentrations, we observed less steady state levels of the HmuUV-T complex (Fig. 6, *state II*, inhibition by substrate). At this point it is difficult to determine whether this is a result of inhibition of association or acceleration of dissociation. Heme is a very hydrophobic and "sticky" compound, and its detrimental effects on the Biacore's microfluidics prevented more extensive characterization. HmuT is unique in the sense that it binds two heme molecules in its central binding site (40). The first binding event is of very high affinity ($K_D = 0.29 \times 10^{-9}$ M), and the second heme molecule binds with a 100-fold reduced affinity ($K_D = 29 \times 10^{-9}$ M) (40). It is therefore tempting to propose that the second binding event (that of the relatively lower affinity) is the one responsible for the observed decrease in complex steady state levels. We currently propose that docking of HmuT leads to structural rearrangements

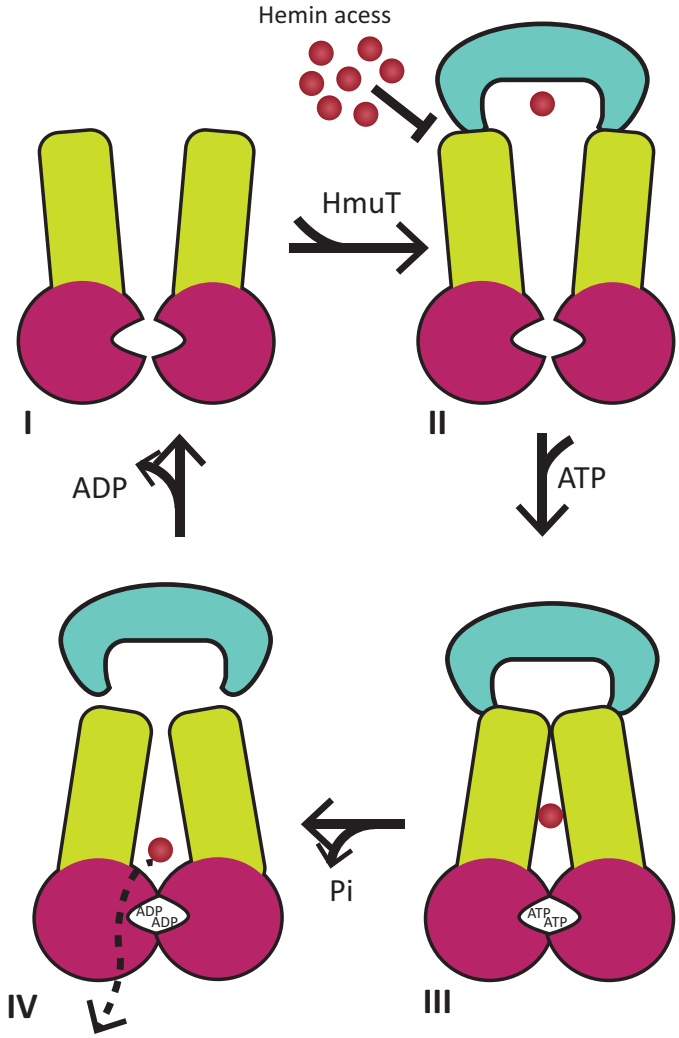

Figure 6. A proposed model for the transport cycle of HnuUV-T. *State I*, in its nucleotide-free state HmuUV is outward-facing. HmuT has the highest affinity to this state and preferentially binds to it. *State II*, a stable complex is formed between HmuUV and HmuT. In the presence of high heme concentrations this interaction is inhibited. *State III*, docking of HmuT and binding of ATP leads to an occluded state. Heme is released from HmuT to the translocation cavity of HmuUV. Binding of ATP is insufficient to dislodge HmuT. *State IV*, ATP hydrolysis proceeds and the hydrolysis products are released, HmuT is dislodged, heme is delivered to the cytoplasm, and the transporter is reset.

in HmuUV: a switch to an inward-facing conformation, and closure of the NBDs dimer that is also facilitated by binding of ATP. ATP binding to the HmuUV-T complex leads to an occluded state where heme is released from HmuT and trapped in the translocation cavity of HmuUV (Fig. 6, *state III*). We currently have no data to support the existence of this conformation, it is inferred from results obtained with BtuCD (46, 47, 53).

Once the stable complex has formed, the heme-binding pocket of HmuT is inaccessible from the outside, and the complex must break for the next transport cycle to take place. In the absence of nucleotide, The HmuUV-T complex has extremely slow dissociation kinetics that are incompatible with a transport cycle. ATP binding *per se* is insufficient to dislocate the tightly docked HmuT, and a transition state is attained where both ATP and HmuT are bound to HmuUV (Fig. 6, *state III*). Relative to two other Type II transporters (BtuCD and MolBC) HmuUV has a lower rate of uncoupled ATP hydrolysis that is stimulated 2–3-fold by HmuT (34, 41, 45, 54, 55). Therefore, once state III is reached hydrolysis now rapidly proceeds, leading to disengagement of HmuT, release of heme to the cytosol, and release of ADP + P_i (Fig. 6, *state IV*). HmuUV is now free of HmuT and of nucleotides. This leads to opening of the NBDs dimer, re-orientation to the outward-facing conformation, and the system is reset (state I).

For several ABC transporters it was demonstrated that the ATPase sites are interdependent, and that ATP hydrolysis follows a "two cylinder" mechanism (45, 56, 57). In such systems, vanadate trapping of one ATPase site disables the other one as well, resulting in a one round of hydrolysis of a single ATP molecule. Very reproducibly we observed that ATP hydrolysis in the presence of vanadate releases exactly half of the amount of HmuT that is released under the complete hydrolyzing conditions (ATP-Mg). This observation suggests that at the population level, hydrolysis of two ATP molecules is statistically required to release 100% of the docked HmuT molecules, whereas one hydrolysis event suffices to release HmuT in 50% of the cases.

The results presented in this report, and the ensuing model, bare much resemblance to those described for BtuCD, yet there are also some differences. For example, the affinity of BtuF to BtuCD is 3–4 orders of magnitude higher than that of HmuT to HmuUV. In addition, the effect of ATP binding and hydrolysis on complex stability is much stronger in HmuUV, whereas in BtuCD the substrate seems to play the more major role. Likewise, BtuCD and MolBC also display mechanistic similarities as well as differences (34, 35). This speciation is also apparent in Type I transporters, where, for example, a single NBD of the histidine transporter (HisPQM) is sufficient to drive transport, whereas in MalFGK this not the case (58, 59). These are just a few examples of many that suggest that the current division to Type I and Type II (29) systems is likely as crude as dividing bacteria to Gram-positive and -negative. To remedy this, more systems need to be systematically studied, both structurally and mechanistically. In conclusion, the results reported herein support the notion that ATP binding (and hydrolysis) serves fundamentally different purposes in Type I and Type II systems. In Type I systems it is required to stabilize unstable complexes, and in Type II systems it is required to break apart stable complexes.

Experimental procedures

Protein expression and purification

HmuUV, MolBC, and BtuCD were expressed and purified essentially as previously described (41, 43, 54). For preparation of membrane fraction, cells were re-suspended in 50 mM Tris-HCl, pH 7.5, 0.5 M NaCl, 30 μg/ml of DNase (Worthington), one complete EDTA-free protease inhibitor mixture tablet (Roche Applied Science), 1 mM $CaCl_2$, 1 mM $MgCl_2$, and ruptured by three passages in an EmulsiFlex-C3 homogenizer (Avestin). Membranes were pelleted by ultracentrifugation at 120,000 × *g* for 45 min, washed, and resuspended in 50 mM Tris-HCl, pH 7.5, 0.5 M NaCl, and 10% (v/v) glycerol, and stored in −80 °C until use. For FLAG-HmuT purification, cells were lysed as before, and following ultracentrifugation at 350,000 × *g*, 30 min, at 4 °C the supernatant was loaded onto an anion-exchange column (Resource Q 1 ml, GE Healthcare). The

unbound fraction, containing HmuT was collected and further purified by size exclusion chromatography (HiLoad 16/600, GE Healthcare). Protein purification was monitored by Coomassie staining of SDS-PAGE and size exclusion chromatography.

SPR measurements

All measurements were performed using a Biacore T200 (GE Healthcare) as extensively as described before (34, 35, 60). His-HmuUV, His-BtuCD, and His-MolBC were immobilized directly onto nickel-nitrilotriacetic acid biosensor chip (GE Healthcare). The running buffer contained 10 mM Tris-HCl, pH 8, 150 mM NaCl, 0.05% *n*-dodecyl-β-D-maltopyranoside. Surface densities were between 0.12 and 0.3 ng/mm^2 (1200–3000 response units for a 150–180-kDa protein-detergent micelle). All injections were performed at least as duplicates in random order and double-referenced. Data analysis was performed using Biacore's standard evaluation software, and a simple 1:1 Langmuir interaction model was used for fitting and derivation of kinetic rate constants.

Association assays in membranes

For preparation of membrane fraction, cells were re-suspended in 50 mM Tris-HCl, pH 7.5, 0.5 M NaCl, 30 μg/ml of DNase (Worthington), one complete EDTA-free protease inhibitor mixture tablet (Roche Applied Science), 1 mM $CaCl_2$, 1 mM $MgCl_2$, and ruptured by tip sonication (3 × 20 s, 600 Watts). Debris and unbroken cells were removed by centrifugation (10 min, 10,000 × *g*) and the membranes were pelleted by ultracentrifugation at 120,000 × *g* for 45 min. The membranes were washed and re-suspended in 50 mM Tris-HCl, pH 7.5, 0.5 M NaCl, and 10% (v/v) glycerol, and stored in −80 °C until use. To incorporate nucleotides in the lumen of the vesicles these were added during the sonication step but omitted from the wash and re-suspension buffers. Purified FLAG-HmuT was added to the membranes at the indicated concentration and the mixture was gently shaken at 4 °C for 30 min. The membrane-bound or unbound fractions were separated by ultracentrifugation at 130,000 × *g* for 15 min, and the membrane fractions were solubilized in equal volumes of 2% SDS. The amount of FLAG-HmuT was visualized by Western blot detection, using an anti-FLAG antibody (Sigma).

ATP hydrolysis

ATP hydrolysis was measured using Molecular Probes EnzCheck kit, at 28 °C, in a 96-well format, according to the manufacturer's specifications. To initiate hydrolysis, 2 mM $MgCl_2$ was injected to a solution containing 0.5 μM HmuUV in 10 mM Tris-HCl, pH 8, 150 mM NaCl, 0.05% *n*-dodecyl-β-D-maltopyranoside, 50 μM EDTA, and the indicated ATP concentration. Where applicable, ADP was added at the indicated concentrations.

Author contributions—O. L. conceived and coordinated the study and wrote the paper. H. Q. A., M. P., and O. L. designed, performed, and analyzed the experiments. N. L. L. provided technical assistance and contributed to the preparation of the figures. All authors reviewed the results and approved the final version of the manuscript.

Acknowledgment—Plasmids for HmuUV and HmuT expression were a kind gift from Kaspar Locher.

References

1. Bateman, A., Birney, E., Durbin, R., Eddy, S. R., Howe, K. L., and Sonnhammer, E. L. (2000) The Pfam protein families database. *Nucleic Acids Res.* **28,** 263–266
2. Berman, H. M., Westbrook, J., Feng, Z., Gilliland, G., Bhat, T. N., Weissig, H., Shindyalov, I. N., and Bourne, P. E. (2000) The Protein Data Bank. *Nucleic Acids Res.* **28,** 235–242
3. Higgins, C. F. (1992) ABC transporters: from microorganisms to man. *Annu. Rev. Cell Biol.* **8,** 67–113
4. Henikoff, S., Greene, E. A., Pietrokovski, S., Bork, P., Attwood, T. K., and Hood, L. (1997) Gene families: the taxonomy of protein paralogs and chimeras. *Science* **278,** 609–614
5. Gottesman, M. M., and Ambudkar, S. V (2001) Overview: ABC transporters and human disease. *J. Bioenerg. Biomembr.* **33,** 453–458
6. Holland, I. B., Cole, S. P. C., Kuchler, K., and Higgins, C. F. (eds)(2003) *ABC proteins: from Bacteria to Man*, Academic Press, New York
7. Ames, G. F., Mimura, C. S., Holbrook, S. R., and Shyamala, V. (1992) Traffic ATPases: a superfamily of transport proteins operating from *Escherichia coli* to humans. *Adv. Enzymol. Relat. Areas Mol. Biol.* **65,** 1–47
8. Dassa, E., and Bouige, P. (2001) The ABC of ABCs: a phylogenetic and functional classification of ABC systems in living organisms. *Res. Microbiol.* **152,** 211–229
9. Davidson, A. L., Dassa, E., Orelle, C., and Chen, J. (2008) Structure, function, and evolution of bacterial ATP-binding cassette systems. *Microbiol. Mol. Biol. Rev.* **72,** 317–364
10. Møller, S. G., Kunkel, T., and Chua, N.-H. (2001) A plastidic ABC protein involved in intercompartmental communication of light signaling. *Genes Dev.* **15,** 90–103
11. Paytubi, S., Wang, X., Lam, Y. W., Izquierdo, L., Hunter, M. J., Jan, E., Hundal, H. S., and Proud, C. G. (2009) ABC50 promotes translation initiation in mammalian cells. *J. Biol. Chem.* **284,** 24061–24073
12. Gottesman, M. M., Fojo, T., and Bates, S. E. (2002) Multidrug resistance in cancer: role of ATP-dependent transporters. *Nat. Rev. Cancer* **2,** 48–58
13. Cole, S. P., Bhardwaj, G., Gerlach, J. H., Mackie, J. E., Grant, C. E., Almquist, K. C., Stewart, A. J., Kurz, E. U., Duncan, A. M., and Deeley, R. G. (1992) Overexpression of a transporter gene in a multidrug-resistant human lung cancer cell line. *Science* **258,** 1650–1654
14. Jones, P. M., and George, A. M. (2005) Multidrug resistance in parasites: ABC transporters, P-glycoproteins and molecular modelling. *Int. J. Parasitol.* **35,** 555–566
15. McDevitt, C. A., Ogunniyi, A. D., Valkov, E., Lawrence, M. C., Kobe, B., McEwan, A. G., and Paton, J. C. (2011) A molecular mechanism for bacterial susceptibility to zinc. *PLoS Pathog.* **7,** e1002357
16. Gat, O., Mendelson, I., Chitlaru, T., Ariel, N., Altboum, Z., Levy, H., Weiss, S., Grosfeld, H., Cohen, S., and Shafferman, A. (2005) The solute-binding component of a putative Mn(II) ABC transporter (MntA) is a novel *Bacillus anthracis* virulence determinant. *Mol. Microbiol.* **58,** 533–551
17. Remy, L., Carrière, M., Derré-Bobillot, A., Martini, C., Sanguinetti, M., and Borezée-Durant, E. (2013) The *Staphylococcus aureus* Opp1 ABC transporter imports nickel and cobalt in zinc-depleted conditions and contributes to virulence. *Mol. Microbiol.* **87,** 730–743
18. Haber, A., Friedman, S., Lobel, L., Burg-Golani, T., Sigal, N., Rose, J., Livnat-Levanon, N., Lewinson, O., and Herskovits, A. A. (2017) L-glutamine induces expression of *Listeria monocytogenes* virulence genes. *PLOS Pathog.* **13,** e1006161
19. Vigonsky, E., Fish, I., Livnat-Levanon, N., Ovcharenko, E., Ben-Tal, N., and Lewinson, O. (2015) Metal binding spectrum and model structure of the *Bacillus anthracis* virulence determinant MntA. *Metallomics* **7,** 1407–1419
20. Karpowich, N. K., Huang, H. H., Smith, P. C., and Hunt, J. F. (2003) Crystal structures of the BtuF periplasmic-binding protein for vitamin B12 suggest a functionally important reduction in protein mobility upon ligand binding. *J. Biol. Chem.* **278,** 8429–8434

21. Bulut, H., Moniot, S., Licht, A., Scheffel, F., Gathmann, S., Saenger, W., and Schneider, E. (2012) Crystal structures of two solute receptors for L-cystine and L-cysteine, respectively, of the human pathogen *Neisseria gonorrhoeae*. *J. Mol. Biol.* **415,** 560–572
22. Schneider, E., Eckey, V., Weidlich, D., Wiesemann, N., Vahedi-Faridi, A., Thaben, P., and Saenger, W. (2012) Receptor-transporter interactions of canonical ATP-binding cassette import systems in prokaryotes. *Eur. J. Cell Biol.* **91,** 311–317
23. Wuttge, S., Bommer, M., Jäger, F., Martins, B. M., Jacob, S., Licht, A., Scheffel, F., Dobbek, H., and Schneider, E. (2012) Determinants of substrate specificity and biochemical properties of the *sn*-glycerol-3-phosphate ATP binding cassette transporter (UgpB-AEC2) of *Escherichia coli*. *Mol. Microbiol.* **86,** 908–920
24. Berntsson, R. P., Smits, S. H., Schmitt, L., Slotboom, D.-J., and Poolman, B. (2010) A structural classification of substrate-binding proteins. *FEBS Lett.* **584,** 2606–2617
25. ter Beek, J., Guskov, A., and Slotboom, D. J. (2014) Structural diversity of ABC transporters. *J. Gen. Physiol.* **143,** 419–435
26. Rees, D. C., Johnson, E., and Lewinson, O. (2009) ABC transporters: the power to change. *Nat. Rev. Mol. Cell Biol.* **10,** 218–227
27. Hollenstein, K., Dawson, R. J., and Locher, K. P. (2007) Structure and mechanism of ABC transporter proteins. *Curr. Opin. Struct. Biol.* **17,** 412–418
28. Locher, K. P. (2016) Mechanistic diversity in ATP-binding cassette (ABC) transporters. *Nat. Struct. Mol. Biol.* **23,** 487–493
29. Lewinson, O., and Livnat-Levanon, N. (2017) Mechanism of action of ABC importers: conservation, divergence, and physiological adaptations. *J. Mol. Biol.* **429,** 606–619
30. Chen, J. (2013) Molecular mechanism of the Escherichia coli maltose transporter. *Curr. Opin. Struct. Biol.* **23,** 492–498
31. Kerppola, R. E., Shyamala, V. K., Klebba, P., and Ames, G. F. (1991) The membrane-bound proteins of periplasmic permeases form a complex: identification of the histidine permease HisQMP complex. *J. Biol. Chem.* **266,** 9857–9865
32. van der Heide, T., and Poolman, B. (2000) Osmoregulated ABC-transport system of *Lactococcus lactis* senses water stress via changes in the physical state of the membrane. *Proc. Natl. Acad. Sci. U.S.A.* **97,** 7102–7106
33. Oldham, M. L., Khare, D., Quiocho, F. A., Davidson, A. L., and Chen, J. (2007) Crystal structure of a catalytic intermediate of the maltose transporter. *Nature* **450,** 515–521
34. Vigonsky, E., Ovcharenko, E., and Lewinson, O. (2013) Two molybdate/tungstate ABC transporters that interact very differently with their substrate binding proteins. *Proc. Natl. Acad. Sci. U.S.A.* **110,** 5440–5445
35. Lewinson, O., Lee, A. T., Locher, K. P., and Rees, D. C. (2010) A distinct mechanism for the ABC transporter BtuCD-F revealed by the dynamics of complex formation. *Nat. Struct. Mol. Biol.* **17,** 332–338
36. Korkhov, V. M., Mireku, S. A., Veprintsev, D. B., and Locher, K. P. (2014) Structure of AMP-PNP-bound BtuCD and mechanism of ATP-powered vitamin B12 transport by BtuCD-F. *Nat. Struct. Mol. Biol.* **21,** 1097–1099
37. Rice, A. J., Alvarez, F. J., Schultz, K. M., Klug, C. S., Davidson, A. L., and Pinkett, H. W. (2013) EPR spectroscopy of MolB2C2-a reveals mechanism of transport for a bacterial type II molybdate importer. *J. Biol. Chem.* **288,** 21228–21235
38. Naoe, Y., Nakamura, N., Doi, A., Sawabe, M., Nakamura, H., Shiro, Y., and Sugimoto, H. (2016) Crystal structure of bacterial haem importer complex in the inward-facing conformation. *Nat. Commun.* **7,** 13411
39. Thompson, J. M., Jones, H. A., and Perry, R. D. (1999) Molecular characterization of the hemin uptake locus (hmu) from *Yersinia pestis* and analysis of hmu mutants for hemin and hemoprotein utilization. *Infect. Immun.* **67,** 3879–3892
40. Mattle, D., Zeltina, A., Woo, J.-S., Goetz, B. A., and Locher, K. P. (2010) Two stacked heme molecules in the binding pocket of the periplasmic heme-binding protein HmuT from *Yersinia pestis*. *J. Mol. Biol.* **404,** 220–231
41. Woo, J.-S., Zeltina, A., Goetz, B. A., and Locher, K. P. (2012) X-ray structure of the *Yersinia pestis* heme transporter HmuUV. *Nat. Struct. Mol. Biol.* **19,** 1310–1315
42. Locher, K. P., Lee, A. T., and Rees, D. C. (2002) The E. coli BtuCD structure: a framework for ABC transporter architecture and mechanism. *Science* **296,** 1091–1098
43. Pinkett, H. W., Lee, A. T., Lum, P., Locher, K. P., and Rees, D. C. (2007) An inward-facing conformation of a putative metal-chelate-type ABC transporter. *Science* **315,** 373–377
44. Borths, E. L., Locher, K. P., Lee, A. T., and Rees, D. C. (2002) The structure of *Escherichia coli* BtuF and binding to its cognate ATP binding cassette transporter. *Proc. Natl. Acad. Sci. U.S.A.* **99,** 16642–16647
45. Tal, N., Ovcharenko, E., and Lewinson, O. (2013) A single intact ATPase site of the ABC transporter BtuCD drives 5% transport activity yet supports full *in vivo* vitamin B12 utilization. *Proc. Natl. Acad. Sci. U.S.A.* **110,** 5434–5439
46. Korkhov, V. M., Mireku, S. A., and Locher, K. P. (2012) Structure of AMP-PNP-bound vitamin B12 transporter BtuCD-F. *Nature* **490,** 367–372
47. Joseph, B., Korkhov, V. M., Yulikov, M., Jeschke, G., and Bordignon, E. (2014) Conformational cycle of the vitamin B12 ABC importer in liposomes detected by double electron-electron resonance (DEER). *J. Biol. Chem.* **289,** 3176–3185
48. Merino, G., Boos, W., Shuman, H. A., and Bohl, E. (1995) The inhibition of maltose transport by the unliganded form of the maltose-binding protein of *Escherichia coli*: experimental findings and mathematical treatment. *J. Theor. Biol.* **177,** 171–179
49. Nguyen, P. T., Li, Q. W., Kadaba, N. S., Lai, J. Y., Yang, J. G., and Rees, D. C. (2015) The contribution of methionine to the stability of the *Escherichia coli* MetNIQ ABC transporter-substrate binding protein complex. *Biol. Chem.* **396,** 1127–1134
50. Davidson, A. L., Shuman, H. A., and Nikaido, H. (1992) Mechanism of maltose transport in *Escherichia coli*: transmembrane signaling by periplasmic binding proteins. *Proc. Natl. Acad. Sci. U.S.A.* **89,** 2360–2364
51. Chen, J., Sharma, S., Quiocho, F. A., and Davidson, A. L. (2001) Trapping the transition state of an ATP-binding cassette transporter: evidence for a concerted mechanism of maltose transport. *Proc. Natl. Acad. Sci. U.S.A.* **98,** 1525–1530
52. Rohrbach, M. R., Braun, V., and Köster, W. (1995) Ferrichrome transport in *Escherichia coli* K-12: altered substrate specificity of mutated periplasmic FhuD and interaction of FhuD with the integral membrane protein FhuB. *J. Bacteriol.* **177,** 7186–7193
53. Joseph, B., Jeschke, G., Goetz, B. A., Locher, K. P., and Bordignon, E. (2011) Transmembrane gate movements in the type II ATP-binding cassette (ABC) importer BtuCD-F during nucleotide cycle. *J. Biol. Chem.* **286,** 41008–41017
54. Borths, E. L., Poolman, B., Hvorup, R. N., Locher, K. P., and Rees, D. C. (2005) *In vitro* functional characterization of BtuCD-F, the *Escherichia coli* ABC transporter for vitamin B12 uptake. *Biochemistry.* **44,** 16301–16309
55. Livnat-Levanon, N., I Gilson, A., Ben-Tal, N., and Lewinson, O. (2016) The uncoupled ATPase activity of the ABC transporter BtuC2D2 leads to a hysteretic conformational change, conformational memory, and improved activity. *Sci. Rep.* **6,** 21696
56. Davidson, A. L., Laghaeian, S. S., and Mannering, D. E. (1996) The maltose transport system of *Escherichia coli* displays positive cooperativity in ATP hydrolysis. *J. Biol. Chem.* **271,** 4858–4863
57. van Veen, H. W., Margolles, A., Müller, M., Higgins, C. F., and Konings, W. N. (2000) The homodimeric ATP-binding cassette transporter LmrA mediates multidrug transport by an alternating two-site (two-cylinder engine) mechanism. *EMBO J.* **19,** 2503–2514
58. Nikaido, K., and Ames, G. F. (1999) One intact ATP-binding subunit is sufficient to support ATP hydrolysis and translocation in an ABC transporter, the histidine permease. *J. Biol. Chem.* **274,** 26727–26735
59. Davidson, A. L., and Sharma, S. (1997) Mutation of a single MalK subunit severely impairs maltose transport activity in *Escherichia coli*. *J. Bacteriol.* **179,** 5458–5464
60. Livnat Levanon, N., Vigonsky, E., and Lewinson, O. (2014) Real time measurements of membrane protein:receptor interactions using surface plasmon resonance (SPR). *J. Vis. Exp.* **93,** e51937